ELSEVIER

Carbohydrate Research 288 (1996) 57–74

CARBOHYDRATE RESEARCH

Predicting helical structures of the exopolysaccharide produced by *Lactobacillus sake* 0-1

Gerard W. Robijn [a,b], Anne Imberty [c], Dick J.C. van den Berg [d], Aat M. Ledeboer [d], Johannis P. Kamerling [a], Johannes F.G. Vliegenthart [a], Serge Pérez [b,*]

[a] *Bijvoet Center, Department of Bio-Organic Chemistry, Utrecht University, P.O. Box 80.075, NL-3508 TB Utrecht, The Netherlands*

[b] *Ingénierie Moléculaire, Institut National de la Recherche Agronomique, BP 1627, 44316 Nantes Cédex 03, France*

[c] *Laboratoire de Synthèse Organique – CNRS, Faculté des Sciences, 2 Rue de la Houssinière, 44072 Nantes Cédex 03, France*

[d] *Unilever Research Laboratory Vlaardingen, P.O. Box 114, NL-3130 AC Vlaardingen, The Netherlands*

Received 8 January 1996; accepted 9 April 1996

Abstract

The viscous exopolysaccharide (EPS) produced by *Lactobacillus sake* 0-1 is a high molecular mass polymer (M_m 6×10^6 Da) consisting of pentasaccharide repeating units with a composition of D-glucose, L-rhamnose, and *sn*-glycerol 3-phosphate in molar ratios of 3:2:1. One of the rhamnose residues in the repeating unit is partially 2-*O*-acetylated. The *O*-deacetylated, deglycerophosphorylated EPS has been investigated by molecular mechanics calculations. A complete conformational analysis of each of the constituent disaccharide fragments has been performed using the flexible residue approach with the MM3(92) force field. Furthermore, using the same force field, CICADA analyses were accomplished on hexa- and octasaccharide substructures of the polysaccharide. Based on these analyses, insight was obtained into nine conformational minima for the polysaccharide. The low energy conformations found by CICADA were extrapolated to regular polysaccharide structures using a polysaccharide builder program. The generated helices exhibit either 2-fold or 3- or 4-fold righthanded chiralities, and in each case the helices are highly extended. © 1996 Elsevier Science Ltd.

* Corresponding author.

0008-6215/96/$15.00
PII S0008-6215(96)00098-5

Keywords: Lactic acid bacteria; Exopolysaccharide; Molecular mechanics; Molecular modelling; Helical structures

1. Introduction

In the food industry, bacterial exopolysaccharides (EPSs) are extensively used as thickening, gelling, and stabilizing agents [1]. Recently, a growing interest has developed in exopolysaccharides from lactic acid bacteria. These 'green' polysaccharides may form a new generation of food thickeners, because they are produced by food grade microorganisms. In this context, structural studies have been carried out on several EPSs produced by lactic acid bacteria [2–9]. One of these biopolymers, namely the EPS produced by *Lactobacillus sake* 0-1, was found to have viscose forming properties that are comparable to those of xanthan gum [10]. This EPS is composed of pentasaccharide repeating units with the following primary structure [8]:

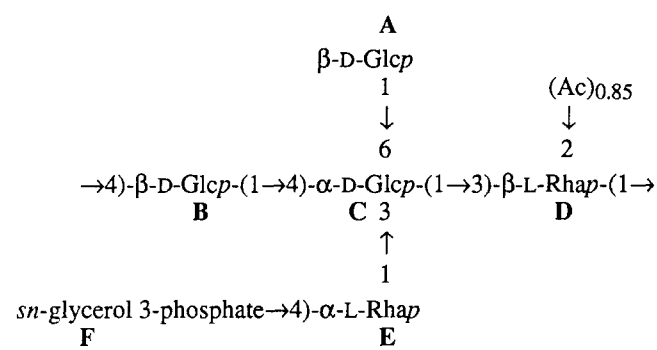

In order to obtain insight into the relationship between the rheological properties of a polysaccharide and its three-dimensional structure, detailed knowledge of the conformational behaviour of such a polysaccharide is essential. To this end, the *O*-deacetylated, deglycerophosphorylated EPS of *Lb. sake* 0-1 was examined through molecular mechanics. The choice for studying the *O*-deacetylated, deglycerophosphorylated material instead of the native EPS was made because for the former polysaccharide good quality NMR data were obtained. Relaxed residue calculations using the MM3(92) force field [11] were performed for each of the constituent disaccharides in the EPS. Using CICADA [12,13], a program to explore the conformational space of flexible molecules, a hexasaccharide as well as an octasaccharide substructure of the EPS have been studied.

From the conformational minima found by these studies, integral helical structures were generated and characterized using a polysaccharide builder program.[1] Physical properties of polysaccharide chains in solution result from specific conformational behavior. Polysaccharide chains have to undergo some topological rearrangements from

[1] S.B. Engelsen, S. Cros, W. Mackie, and S. Pérez, unpublished results.

disordered random coils to more ordered conformations favorable to intermolecular interactions and associations. Spatial organization of the constituting units, within the polysaccharide chain, can be well defined by consecutive fragments having orientations characterized by the helical parameters (n, h). In such cases, helical parameters have to be considered on a local basis. For the sake of comparing different secondary structures, it is appropriate to use 'ideal' integral helices as characterized by their helical parameters.

2. Experimental

Nomenclature.—The dihedral angles of the glycosidic linkages of a disaccharide fragment A(1 → x)B are defined as $\phi = \Theta(\text{O-5}_A\text{–C-1}_A\text{–O-}x_B\text{–C-}x_B)$, and $\psi = \Theta(\text{C-1}_A\text{–O-}x_B\text{–C-}x_B\text{–C-}(x+1)_B)$. In the case of a 1 → 6 linkage, the third glycosidic torsion is defined as $\omega = \Theta(\text{O-1}_A\text{–C-6}_B\text{–C-5}_B\text{–O-5}_B)$. The dihedral angles of exocyclic hydroxymethyl groups are defined as Θ(O-6–C-6–C-5–O-5). The signs of the torsion angles are in agreement with the IUPAC-IUB conventions [14]. The 10 possible classes of geometrical orientations that a dihedral angle can adopt can be described by a one-letter code as indicated in Fig. 1 [13].

MM3 calculations on disaccharide methyl glycosides.—The MM3 force field (version May 1992) [11,15] was used to generate relaxed maps for each of the constituent disaccharide fragments of the *O*-deacetylated, deglycerophosphorylated EPS **1** (Fig. 2). The geometry optimization of this force-field takes into account stretching, bending, stretch–bending, torsional, and dipolar contributions, as well as van der Waals interactions, and a correction for the anomeric effect [11,15]. The MM3 force-field has been demonstrated to be successful for the modelling of many carbohydrates, and it has been shown to reproduce the exoanomeric effect well [16].

For each of the disaccharides α-D-Glc*p*-(1 → 3)-β-L-Rha*p*-OMe (**C** → **D**), β-L-Rha*p*-(1 → 4)-β-D-Glc*p*-OMe (**D** → **B**), and α-L-Rha*p*-(1 → 3)-α-D-Glc*p*-OMe (**E** → **C**) eight combinations of exocyclic orientations were used as starting geometries. These include clockwise (c) and anticlockwise (r) orientations of the hydroxyl groups [17,18], and gauche–gauche (gg) and gauche–trans (gt) orientations of the glucose ω angle

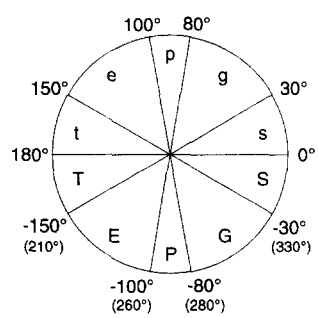

Fig. 1. One-letter code for dihedral angle values according to ref. [13].

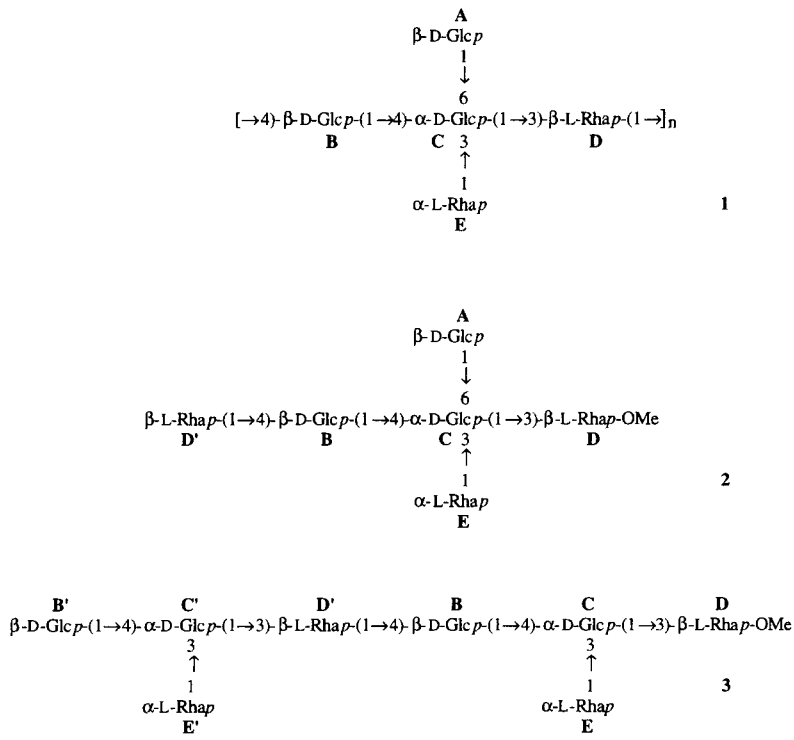

Fig. 2. Structures and residue labeling of the *O*-deacetylated, deglycerophosphorylated EPS (**1**), and of hexasaccharide (**2**) and octasaccharide (**3**) substructures of **1**.

(O-6–C-6–C-5–O-5). Likewise, for the disaccharide β-D-Glc *p*-(1 → 4)-α-D-Glc *p*-OMe (**B** → **C**) sixteen starting geometries were considered, taking into account *gg* and *gt* orientations for the ω angles of both glucose residues. For the disaccharide β-D-Glc *p*-(1 → 6)-α-D-Glc *p*-OMe (**A** → **C**) three adiabatic maps were calculated, reflecting a *gg*, *gt*, or *tg* orientation around the glycosidic ω angle. In each case, four starting conformations were used (*cc*, *cr*, *rc*, and *rr*), in which the ω angle of the non-reducing glucose residue was set to a *gt* orientation. The *gg* and *tg* orientations were not considered, since it has been demonstrated that all conformational minima found for this disaccharide by MM3(92) have a *gt* orientation around this torsion angle [19].

Prior to the calculation of the relaxed maps, all starting conformers were first optimized by MM3 using the block-diagonal minimization method, which was continued until the energy changed less than $0.00008 \times n$ kcal/mol per 5 iterations, where n is the number of atoms in the structure. The dielectric constant (ε) was set to 4 [16]. The optimized coordinates were used as starting points for the calculation of the corresponding relaxed residue maps. The energies were calculated on a 10° by 10° grid.

CICADA calculations.—A CICADA (Channels In Conformational space Analyzed by Driver Approach) analysis [12,13] was performed on a hexasaccharide substructure **2** (Fig. 2) of EPS **1**. The potential energy hypersurface (PES) of the hexasaccharide was

probed by the CICADA program, using the MM3 force-field. Six starting structures were used as input for the CICADA analysis with different orientations around the ϕ, ψ, and ω angles of the **C** → **D** and **A** → **C** linkages (see Fig. 2), based on the low-energy conformations found in the relaxed maps of the corresponding disaccharides. The different starting structures were first pre-optimized by MM3, using the block-diagonal minimization method as described above. During the CICADA search, all eleven glycosidic torsion angles were driven, as well as the two ω angles of the exocyclic hydroxymethyl groups of residues **A** and **B**. The remaining torsions of the exocyclic hydroxyl groups were only monitored. A search increment of 20° was applied for all driven torsion angles. Two conformations were considered different if one of the driven or monitored angles differed by at least 30°. A relative energy cut-off of 50 kcal/mol was applied for exploring the PES, whereas a relative energy cut-off of 10 kcal/mol was applied for considering a new geometry as a new starting conformer. The search was stopped after 9000 minima on the potential energy surface were found. The total number of MM3 calculations was 41,389. The conformations and transition states found by CICADA were analysed by the PANIC program [13], which explores the paths along the PES. Conformations were clustered into families and their relative populations were calculated, applying a Boltzmann distribution at a temperature of 25 °C. Average interproton distances were calculated on the whole ensemble of conformations (at 25 °C), using r^{-6} dependence for distance averaging, according to [20].

A second CICADA calculation was carried out on an octasaccharide substructure **3** of the polysaccharide (Fig. 2). In this case only the **C′** → **D′** and **C** → **D** glycosidic torsion angles were driven, and all other torsion angles (glycosidic, exocyclic hydroxyl, and exocyclic hydroxymethyl) were monitored. The initial ring geometries and torsion angles of the two starting conformers that were used in this calculation were taken from the energy minima of families 1 and 2 of the hexasaccharide simulation (vide supra). The search was stopped after 3722 minima on the potential energy surface were found. The total number of MM3 calculations was 19,281. An average distance matrix was calculated for the complete ensemble of conformations at 25 °C, using r^{-6} dependence for distance averaging, according to [20].

Generation of helices.—From the conformational minima found by the CICADA analyses, integral helices were generated using a polysaccharide builder program.[2] The helices are described in terms of a set of helical parameters (n, h), n being the number of repeating units per turn of the helix and h being the translation of a single repeating unit along the helical axis. Helices with right-handed chiralities correspond to positive values of n. Conversely, negative values of n correspond to left-handed chiralities. As input for the program, preoptimized monosaccharides from MONOBANK [21] in conjunction with glycosidic torsion angles from minima found by the CICADA analyses were used. The helices were then generated in a two-step procedure. In the first step, helical parameters were calculated and new values for the torsion angles of the backbone residues were determined to arrive at the nearest n-fold helical structure. Secondly, integral helices composed of typically 10 repeating units were generated using the

[2] S.B. Engelsen, S. Cros, W. Mackie, and S. Pérez, unpublished results.

modified torsion angles. In order to produce 'clean' integral helical structures, all glycosidic torsion angles in the backbone of the polysaccharide were allowed to change. Changes never exceeded four degrees per individual modified torsion angle.

NMR spectroscopy.—The *O*-deacetylated, deglycerophosphorylated EPS **1** was exchanged twice in 99.9% D_2O (Isotec) with intermediate lyophilization, and finally

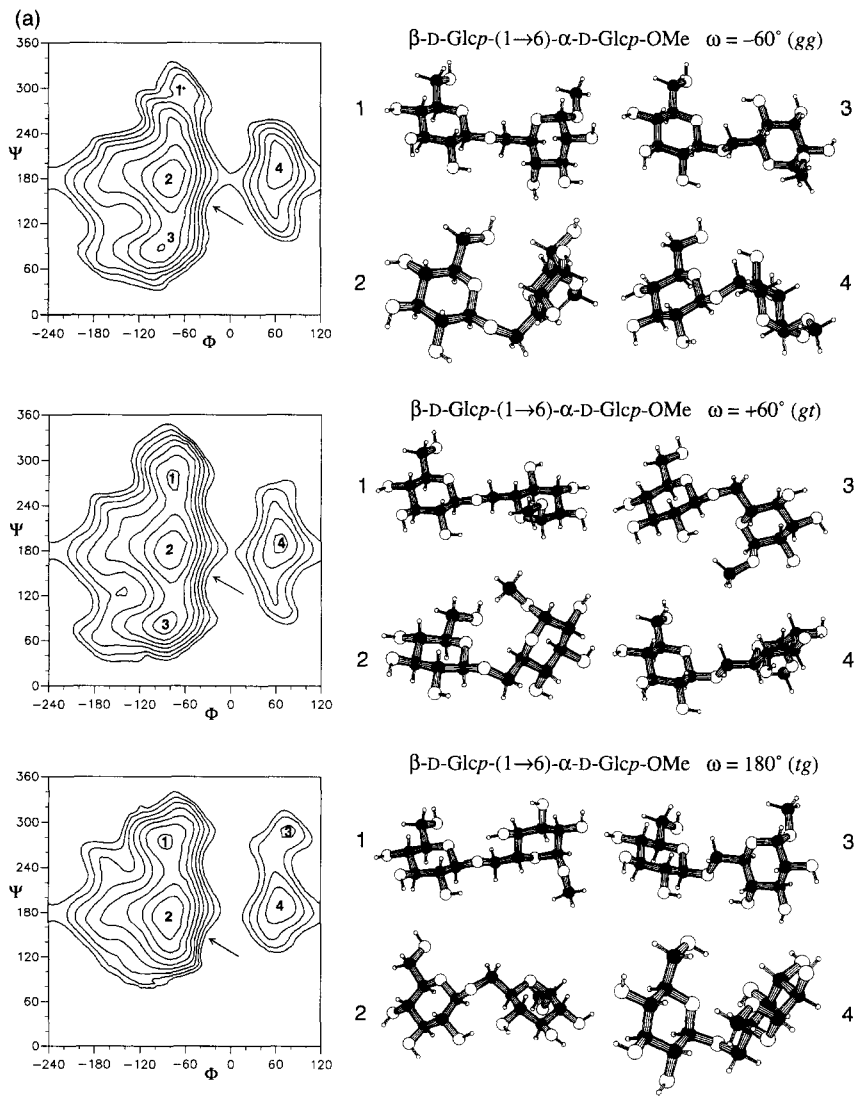

Fig. 3. MM3 adiabatic iso-energy contour plots for each of the 5 constituent disaccharides of the EPS. Contours are plotted at regular intervals of 1 kcal/mol up to 8 kcal/mol with respect to the global energy minimum. Drawings corresponding to the different low-energy conformations are shown. The global minimum in each map is indicated with an arrow.

dissolved in 99.96% D_2O (Isotec). 500 MHz 2D NOESY experiments were performed on a Bruker AMX-500 spectrometer, at a probe temperature of 80 °C, using mixing times of 20, 40, 75, 110, 150, or 200 ms. Spectral widths were 3300 Hz in each dimension. The HOD signal was presaturated for 1 s during the relaxation delay. A homospoil pulse of 5 ms, followed by a recovery of 15 ms was applied during the mixing time. In each case, 512 spectra of 2K data points with 8 scans per t_1 increment were recorded. The data were processed using the TRITON software (Bijvoet Center,

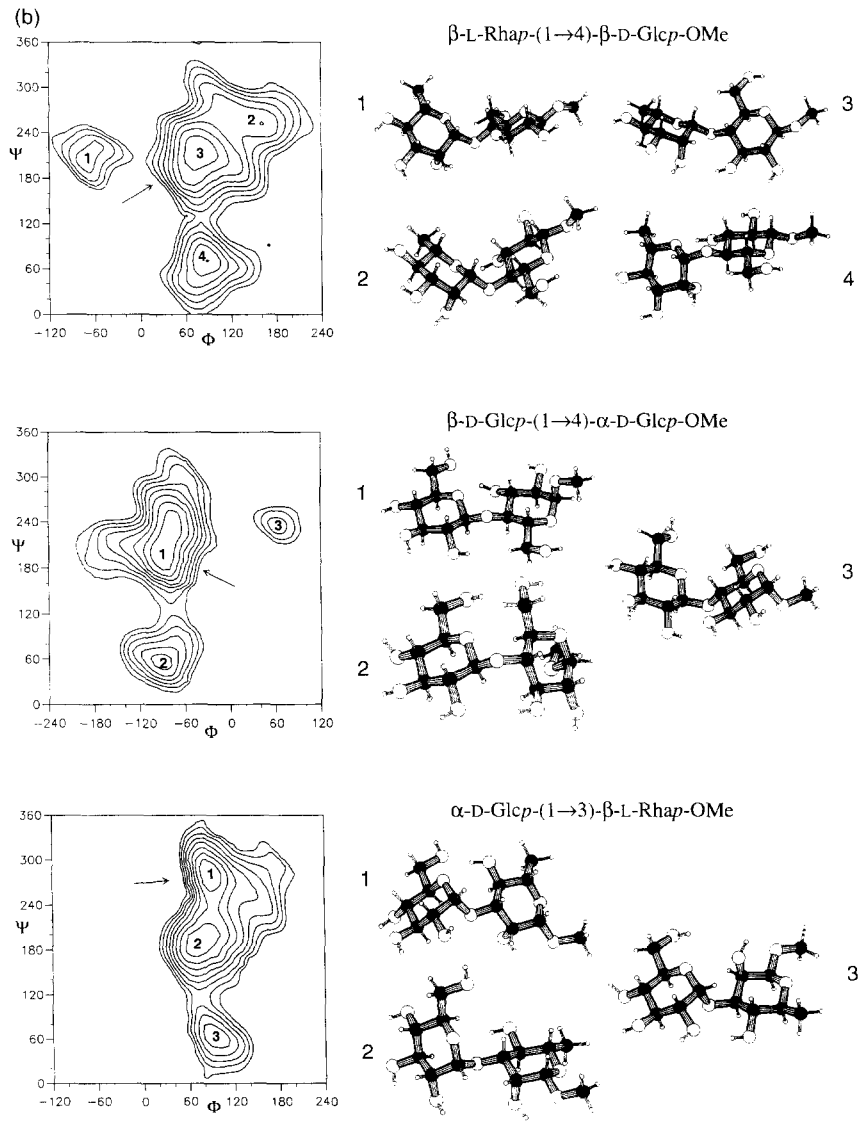

Fig. 3 (continued).

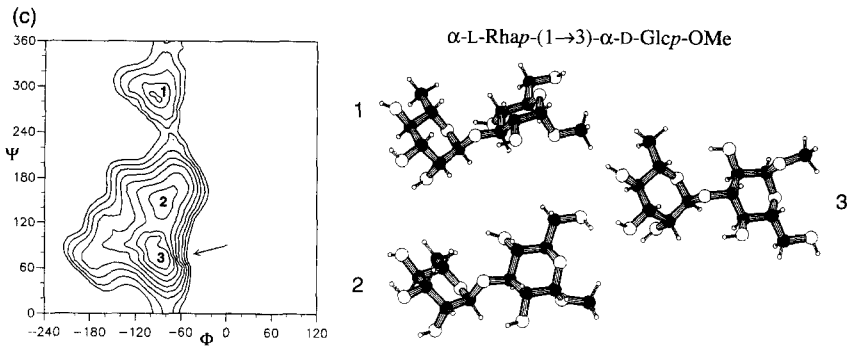

Fig. 3 (continued).

department of NMR spectroscopy). In all spectra, the time-domain data sets were multiplied with a $\pi/3$-shifted sine bell and, after zero-filling and Fourier transformation, data sets of 1024×2048 points were obtained, which were baseline corrected with a fourth order polynomal function in both directions. Cross-peak intensities were integrated within a rectangular area around the peak maximum. Interproton distances were calculated by relating their initial NOE build-up rates to that of intraresidual proton pairs with known distances (e.g. H-1 · · · H-2 for α-D-Glc*p* or H-1 · · · H-3 and H-1 · · · H-5 for β-D-Glc*p* residues) [22,23].

Hardware.—The MM3 calculations were performed on Silicon Graphics Indigo, Indigo2 or Indy workstations. CICADA calculations were performed on a Silicon Graphics Power Challenge computer. The calculations of helical polysaccharide structures were carried out on an IBM 640 workstation. NMR data were processed on Silicon Graphics Indigo or Indigo2 workstations.

3. Results and discussion

Molecular mechanics of disaccharide methyl glycosides.—As a first step in the molecular mechanics analysis of the EPS produced by *Lb. sake* 0-1, fully relaxed energy maps of the five constituent disaccharide fragments of the polysaccharide have been constructed by means of the molecular mechanics force-field MM3(92). In Fig. 3 the adiabatic energy maps are shown as a function of ϕ and ψ for each of the five investigated disaccharides. In every map, the global minimum, as well as the different local energy minima are indicated, along with the corresponding structures. Iso-energy contours have been plotted at regular intervals of 1 kcal/mol up to 8 kcal/mol above the global minimum in each map. The glycosidic torsion angles and the relative energies of the different minima, along with the corresponding starting geometries are given in Table 1. The three adiabatic maps found for methyl α-gentiobioside (β-D-Glc*p*-(1 → 6)-α-D-Glc*p*-OMe) with *gg*, *gt*, and *tg* orientations around the ω angle of the glycosidic bond resemble closely the results found by a more extensive MM3 calculation of this disaccharide [19]. The adiabatic energy map of methyl α-cellobioside [β-D-Glc*p*-(1 →

Table 1
Torsion angles and energies corresponding to the different local minima, extracted from the relaxed energy maps of the disaccharides examined by MM3 (see also Fig. 3)

Disaccharide	Torsion angle		MM3 energy (kcal/mol)	Starting conformer
	ϕ	ψ		
β-D-Glc *p*-(1 → 6)-α-D-Glc *p*-OMe	−80	180	21.97	*gtrr* [a]
gg (ω = −60°)	−90	90	23.89	*gtrc*
	70	200	25.07	*gtrc*
	−60	300	26.89	*gtrc*
β-D-Glc *p*-(1 → 6)-α-D-Glc *p*-OMe	−80	180	21.51	*gtrr*
gt (ω = +60°)	−90	80	22.96	*gtrr*
	−80	280	23.26	*gtrr*
	70	190	25.22	*gtrr*
β-D-Glc *p*-(1 → 6)-α-D-Glc *p*-OMe	−80	180	21.71	*gtrc*
tg (ω = 180°)	−90	280	23.55	*gtrr*
	70	190	25.82	*gtrc*
	80	290	27.42	*gtcc*
β-L-Rha *p*-(1 → 4)-β-D-Glc *p*-OMe	80	220	24.09	*gtrr* [b]
	90	70	26.03	*gtcc*
	160	250	27.03	*gtcc*
	−70	200	28.59	*gtcc*
β-D-Glc *p*-(1 → 4)-α-D-Glc *p*-OMe	−90	200	22.25	*gtgtrc* [c]
	−90	60	24.73	*gtgtcc*
	60	230	27.61	*gtgtrc*
α-D-Glc *p*-(1 → 3)-β-L-Rha *p*-OMe	90	280	24.19	*gtrr* [d]
	70	190	24.33	*gtrr*
	100	60	27.45	*gtcc*
α-L-Rha *p*-(1 → 3)-α-D-Glc *p*-OMe	−90	70	24.23	*gtcc* [e]
	−80	140	25.70	*gtcc*
	−100	290	27.80	*gtcc*

[a,b,d,e] *gtrr* reflects a *gt* conformation for the exocyclic hydroxymethyl groups and an anticlockwise orientation of the exocyclic hydroxyl groups, etc.
[c] *gtgtrc* reflects a *gt* conformation for both exocyclic hyroxymethyl groups, an anticlockwise orientation of the hydroxyl groups of the β-D-glucose residue, and a clockwise orientation of the hydroxyl groups of the α-D-glucose residue, etc.

4)-α-D-Glc *p*-OMe] differs only slightly from earlier MM2 calculations on cellobiose [17,24]. Inspection of the different potential energy surfaces of the three glycosidic linkages that take part in the EPS backbone shows that the α-D-Glc *p*-(1 → 3)β-L-Rha linkage (**C** → **D**) is the most flexible one. In this case, the minima 1 and 2 (Fig. 3) are very close in energy (24.19 and 24.33 kcal/mol, respectively) and the energy barrier between the two minima is only 1.7 kcal/mol.

CICADA analysis.—As a model for the molecular mechanics analysis of the *Lb. sake* 0-1 polysaccharide, hexasaccharide **2** (Fig. 2) was constructed. In order to involve all glycosidic linkages that are also present in the native polysaccharide, **2** includes the repeating unit of the EPS, extended with an extra rhamnose residue. The model compound was investigated using the CICADA program [12,13] which serves as an intelligent shell for the force-field, searching for low-energy regions on the potential

Table 2
Global minima for the 9 most important families found by CICADA for hexasaccharide **2**, and helical parameters for corresponding polysaccharide structures

Family	Torsion angles [a]						Relative energy (kcal/mol)	Boltzmann population (%) [c]	Helical parameters [d]	
	A → C	**D′ → B**	**B → C**	**C → D**	**E → C**	H.M. [b]			*n*	*h* (nm)
1	Gtg	gE	GE	pP	Ge	g g	0.00	57.4	2	1.481
2	Gtg	gE	GE	pT	Ge	g g	0.93	11.2	+3	1.444
3	Geg	gE	GE	gT	Ge	g g	1.18	6.6	+4	1.366
4	Geg	gE	GE	pP	Ge	g g	1.52	8.0	2	1.480
5	GTG	gE	GE	pT	Pe	g g	1.67	6.1	+3	1.439
6	GTG	gE	GE	pG	Pe	g g	1.93	4.3	2	1.465
7	Gtt	gE	GE	pT	Ge	g g	2.16	2.8	+3	1.443
8	GPg	gE	GE	pT	Pe	g g	2.56	1.1	+3	1.443
9	Ptt	gE	GE	pG	Gt	g g	2.67	1.0	2	1.479

[a] One-letter code (see Fig. 1) for the torsion angles of the different glycosidic linkages. For each linkage the codes for ϕ, ψ (and ω) are given, respectively.
[b] H.M. = hydroxymethyl; the first letter corresponds to the ω angle of the exocyclic hydroxymethyl group of residue **A**, and the second to residue **B**.
[c] At 25 °C.
[d] n = Number of repeating units per helical turn; h = helical repeat advancement (nm), determined for the closest integral helix.

energy hypersurface (PES), thereby saving a considerable amount of computational time, when compared to the traditional grid search. The CICADA approach has recently succeeded in finding the various minima of a number of carbohydrates [13,25–27].

The complete ensemble of conformations resulting from the CICADA analysis has been clustered into different conformational families, within an energy window of 5 kcal/mol above the global minimum. Nine families were found to have relative Boltzmann populations of at least 1.0%. For each of these families, the lowest energy conformation is listed in Table 2, along with the corresponding torsion angles for all glycosidic linkages and exocyclic hydroxymethyl groups according to the one-letter code as shown in Fig. 1. The relative energies and relative populations based on a Boltzmann weighted distribution (at 25 °C) are also indicated in Table 2. In Fig. 4 all conformers less than 8 kcal/mol above the global minimum are plotted, superimposed on the corresponding disaccharide relaxed map. Fig. 4 indicates that most of the local minima that are present in the corresponding disaccharide fragments are also present on the PES of hexasaccharide **2** as determined by CICADA. In Fig. 5A the minimum energy structures of each of the nine major families have been fitted onto the internal

Fig. 4. Plots of the complete ensemble of conformers found by CICADA for hexasaccharide **2** as a function of ϕ and ψ for each of the different glycosidic linkages in the polysaccharide, superimposed on the corresponding MM3 disaccharide maps. Iso-energy contours (for the disaccharides) and conformers (for hexasaccharide **2**) have been plotted up to 8 kcal/mol above the global minimum in each case. Legend (see also Fig. 2): (I) **A → C** ($\omega = -60°$); (II) **A → C** ($\omega = +60°$); (III) **A → C** ($\omega = 180°$); (IV) **D′ → B**; (V) **B → C**; (VI) **C → D**; (VII) **E → C**.

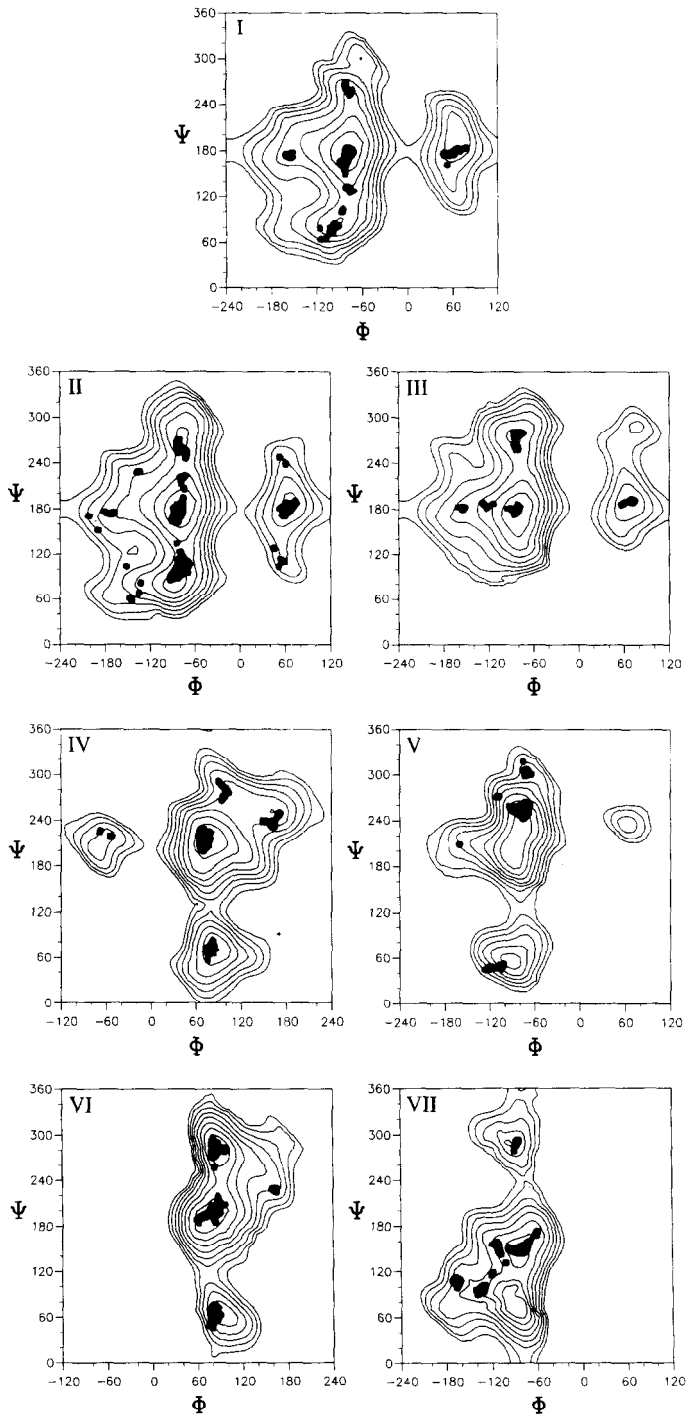
I
II
III
IV
V
VI
VII
Ψ
Φ
360
300
240
180
120
60
0
−240 −180 −120 −60 0 60 120
−120 −60 0 60 120 180 240

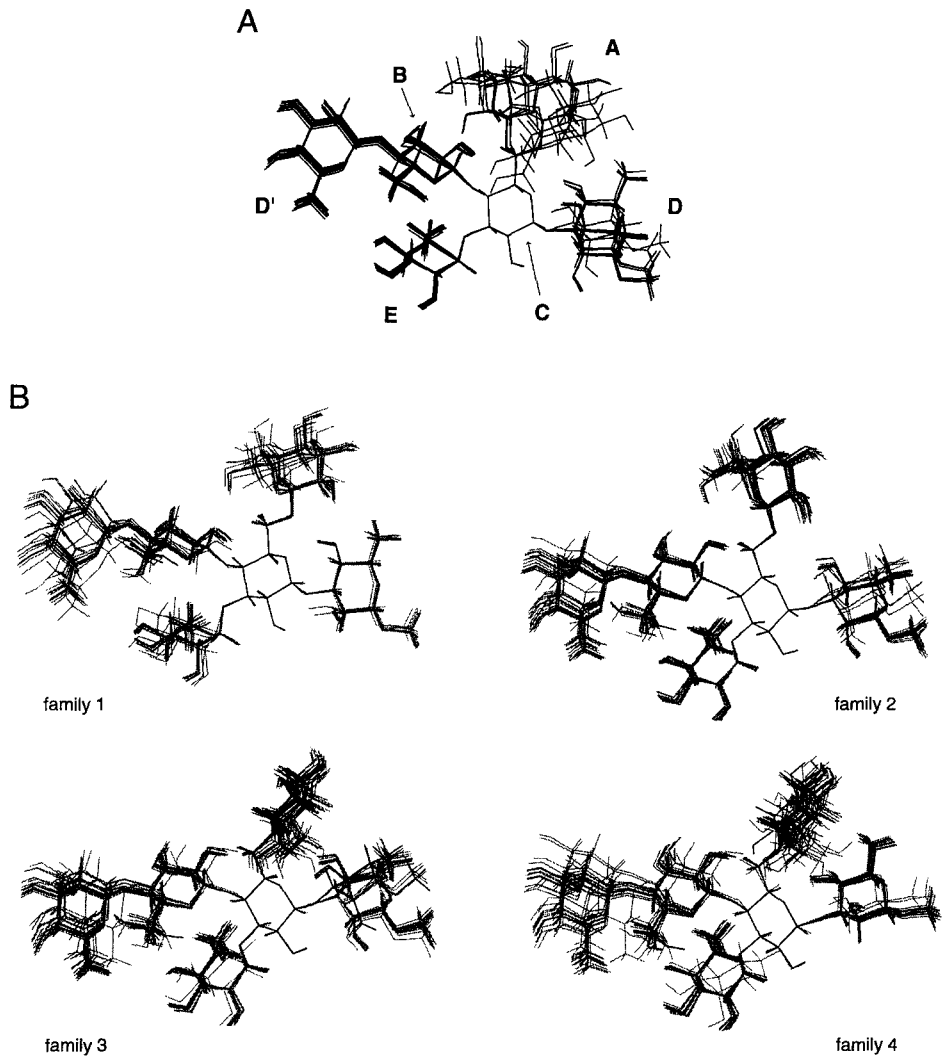

Fig. 5. (A) Superposition of the lowest-energy conformers of the nine most important conformational families found by CICADA for hexasaccharide **2**, fitted on the internal α-D-glucosyl residues **C**. Residue labeling according to Fig. 2 is indicated. (B) Drawings of the lowest-energy conformers (black) of each of the families 1, 2, 3, and 4, along with conformers within the same families (grey), using an energy cut-off of 5 kcal/mol.

α-glucosyl residue **C**, displaying the low-energy conformational possibilities for **2**. In Fig. 5B, for each of the families 1, 2, 3, and 4 the global minimum has been plotted, along with a number of structures that were clustered in the same family. This displays the extent of conformational freedom within each individual family.

It is evident from Table 2 and Fig. 5A that in **D'** → **B**, **B** → **C**, and **C** → **D**, the **C** → **D** linkage is the major origin of flexibility. In each of the families, the conforma-

Table 3
Absolute flexibilities for the different glycosidic torsion angles of hexasaccharide **2**, as determined on the complete ensembles of conformations found by CICADA

Glycosidic torsion	**A → C**			**D′ → B**		**B → C**		**C → D**		**E → C**	
	ϕ	ψ	ω	ϕ	ψ	ϕ	ψ	ϕ	ψ	ϕ	ψ
Absolute flexibility ($\times 10^{-5}$) at 298 K	0.22	1.82	0.41	0.13	0.12	0.13	0.22	0.27	4.19	0.11	0.10

tion around the **D′ → B** linkage is found to be gE, and for the **B → C** linkage only GE conformations are observed. However, for the **C → D** linkage pP (families 1 and 4; total population 65.4%), as well as pT (families 2, 5, 7, and 8), gT (family 3), and pG (families 6 and 9) conformations were found. The two side-chain linkages **A → C** and **E → C** appear to have a different conformational behaviour with respect to one another as well (Table 2; Fig. 5A). The **A → C** linkage is very flexible, adopting predominantly Gtg, Geg, and GTG conformations. Conversely, the **E → C** linkage is relatively rigid, adopting mainly Ge (86.0%) or Pe conformations.

A flexibility analysis, performed on the complete ensemble of glycosidic torsion angles, using the PANIC program [13] generates 'absolute flexibility values' that can be considered as measures for the lowest-energy conformational interconversions. These flexibility values decrease when energy barriers increase and vice versa [12]. Absolute flexibility values for each of the glycosidic torsion angles in **2** are presented in Table 3. The 1,6-linked β-D-glucosyl side-chain residue (**A → C**) is very flexible, primarily due to the conformational freedom of the ψ angle (flexibility value 1.82). On the contrary, the 1,3-linked α-L-rhamnosyl side-chain residue (**E → C**) appears to be very restricted, having flexibility values of 0.11 and 0.10 for the ϕ and ψ angles, respectively. Within the backbone of the polysaccharide, as demonstrated above, the **C → D** linkage is the most flexible, owing to the high flexibility of the ψ angle (flexibility value 4.19). The other backbone linkages **D′ → B** and **B → C** are much more rigid (flexibility values 0.12–0.22).

In order to verify that conformational changes in the backbone of the polysaccharide occur primarily at the highly flexible **C → D** linkage, and to ensure that the finding of such a flexible **C → D** linkage in the analysis of **2** was not a misleading result due to an 'end-effect' (because in **2** Rha **D** is located in a terminal position), a larger model oligosaccharide (octasaccharide **3**, Fig. 2) was examined by CICADA. The 1,6-linked β-D-glucosyl side-chains were not included in the analysis of **3**, based on the assumption that the flexible **A → C** linkages do not significantly influence the backbone conformation of the polysaccharide, and thereby saving computational time. Furthermore, since the objective of the CICADA analysis of **3** was merely an evaluation of the α-D-Glc*p*-(1 → 3)-β-L-Rha*p* linkage, for the sake of computational time only the torsion angles of the **C′ → D′** and **C → D** linkages were driven. From Table 4 it is clear that both linkages **C′ → D′** and **C → D** behave similarly, adopting pP or pT conformations (corresponding to the energy minima 1 and 2 on the α-D-Glc*p*-(1 → 3)-β-L-Rha*p*-OMe disaccharide map, respectively; see Fig. 3). Furthermore, the absolute flexibility values of the torsion angles of both glycosidic linkages are similar (Table 4).

Table 4
Global minima for the 4 most important families found by CICADA for octasaccharide **3**, and helical parameters for corresponding polysaccharide structures. Absolute flexibilities for the driven glycosidic torsion angles as determined on the complete ensembles of conformations found by CICADA

Family	Torsion angles [a]				Relative energy (kcal/mol)	Boltzmann population (%) [b]	Helical parameters [c]	
	C′ → D′		C → D				*n*	*h* (nm)
1	pP		pG (pP) [d]		0.00	36.5	+8	2.405
2	pP		pT		0.10	21.9	−5	1.908
3	pT		pP		0.11	25.8	−6	1.923
4	pT		pT		0.12	15.7	−4	2.824
	ϕ	ψ	ϕ	ψ				
Absolute flexibility ($\times 10^{-5}$) at 298 K	0.86	9.60	1.16	9.67				

[a] One-letter code (see Table 2).
[b] At 25 °C.
[c] *n* = number of repeating units per helical turn; *h* = helical repeat advancement (nm), determined for the closest integral helix.
[d] Formally $\psi_{C \rightarrow D}$ corresponds to a G conformation (286.7°); however, the value is less than 10° different from the P conformations found for the other $\psi_{C \rightarrow D}$ and $\psi_{C' \rightarrow D'}$ angles (277.1°–279.4°).

Distance analysis.—From the complete ensembles of conformations found by the CICADA analyses of **2** and **3**, average interresidue $^{1}H-^{1}H$ distances have been calculated. Furthermore, for the *O*-deacetylated, deglycerophosphorylated EPS (**1**) interresidual $^{1}H-^{1}H$ distances have been estimated from the NOE build-up rates of the corresponding cross-peaks in the 2D NOESY spectra. A simple reference distance method was applied, using strong intraresidue NOE cross-peaks which originate from proton pairs with known distances for distance calibration. It should be noted that the distances determined from the NOE build-up experiments are crude approximations, since this method does not allow for effects caused by differences in internal motion, spin diffusion, anisotropic tumbling or integration errors. The calculated (CICADA) and observed (NOE build-up) distances are collected in Table 5.

Comparison of the calculated and observed interproton distances shows a close agreement for proton pairs corresponding to the **A** → **C**, **D** → **B**, and **E** → **C** linkages. However, a significant difference is found between the calculated and observed **B** H-1,**C** H-4 distances. From the CICADA analysis of **2** it was concluded that primarily GE conformations are occupied around the **B** → **C** linkage, which corresponds to area 1 on the β-D-Glc*p*-(1 → 4)-α-D-Glc*p*-OMe disaccharide map (see Figs. 2 and 3). Notwithstanding, the results from the NOE experiments can only be accommodated when contributions of conformations in area 2 of the iso-energy map (Fig. 2) are considered. However, from NMR studies on methyl cellobioside [28] it was determined that the corresponding H-1 · · · H-4 distance is 0.222 nm, which is in good agreement with the calculated **B** H-1,**C** H-4 distances for **2** and **3** (Table 5).

For the flexible **C** → **D** linkage, four different NOE cross-peaks were identified in the NOESY spectra of **1** (Table 5). The distances determined from the NOE build-up curves

Table 5
Calculated inter-proton distances (from CICADA analysis) for hexasaccharide **2** and octasaccharide **3**, and observed distances (from NOE build-up measurements) for *O*-deacetylated, deglycerophosphorylated EPS **1**

Atom pair	Observed distance (nm)	Calculated distance (nm)	
		2	**3**
D H-1, **B** H-4	0.25	0.25	0.25
B H-1, **C** H-4	0.34	0.24	0.24
B H-1, **C** H-6b [a]	0.24	0.27/0.22	0.27/0.22
C H-1, **D** H-3	0.35	0.23	0.26
C H-1, **D** H-2	0.25	0.26	0.28
C H-5, **D** H-3	0.30	0.39	0.27
C H-5, **D** H-4	0.32	0.29	0.30
E H-1, **C** H-3	0.25	0.25	0.25
E H-6, **B** H-2	0.29	0.29	0.30
A H-1, **C** H-6b [a]	0.28	0.27/0.24	—

[a] Because the resonances **C** H-6a/6b in the ^{1}H NMR spectrum of **1** have not been stereospecifically assigned, calculated distances (for **2** and **3**) from **B** H-1 or **A** H-1 to both **C** H-6pro*R* and **C** H-6pro*S* are given.

of these cross-peaks cannot be accommodated by any single conformation, which is in agreement with the multiple minimum-energy conformations found by the CICADA analyses. When the NOE-derived distances and the distances obtained from the CICADA analyses of **2** and **3** are compared, significant differences are observed for the proton-pairs **C** H-1,**D** H-3 and **C** H-5,**D** H-3. It seems that especially the relatively high contributions of conformers with a pP conformation around the **C** → **D** linkage in the CICADA calculations of the model oligosaccharides **2** and **3** are responsible for this discrepancy. The CICADA analyses of **2** and **3** show a significant difference between the **C** H-5,**D** H-3 interproton distances. Since the low-energy conformations found in the two analyses are very similar with respect to the **C** → **D** linkage, this difference is only due to a subtle difference in population of the various low-energy conformations in the two analyses. Finally, the 'non-sequential' interproton distance **E** H-6, **B** H-2, as determined for **1**, is reproduced by the CICADA analyses of both **2** and **3**.

Generation of helical structures.—From the energy minima of each of the nine families as determined for **2**, stable helices have been generated. Side- and topviews of several polysaccharide structures are shown in Fig. 6A. Helical parameters *n* and *h* are collected in Table 2. The helices generated from families 1, 4, 6, and 9, having a pP or pG conformation around the **C** → **D** linkage, exhibit 2-fold chiralities and are highly extended (*h* 1.465–1.481 nm). These four helical structures (representing a population of 70.7% for **2**) only differ significantly with respect to the conformations of the β-D-glucosyl side-chains (**A** → **C** linkage), being Gtg, Geg, GTG, and Ptt, respectively. From families 2, 5, 7, and 8 (total population 21.2%), which all adopt a pT conformation around the **C** → **D** linkage, 3-fold right-handed helices were generated, which are also highly extended (*h* 1.439–1.444 nm). Finally, family 3 (population 6.6%; gT conformation for the **C** → **D** linkage) has been elongated into a somewhat less extended helical structure (*h* 1.366 nm) with 4-fold right-handed chirality.

Similarly, for **3** helical parameters were established (Table 4) and polysaccharide

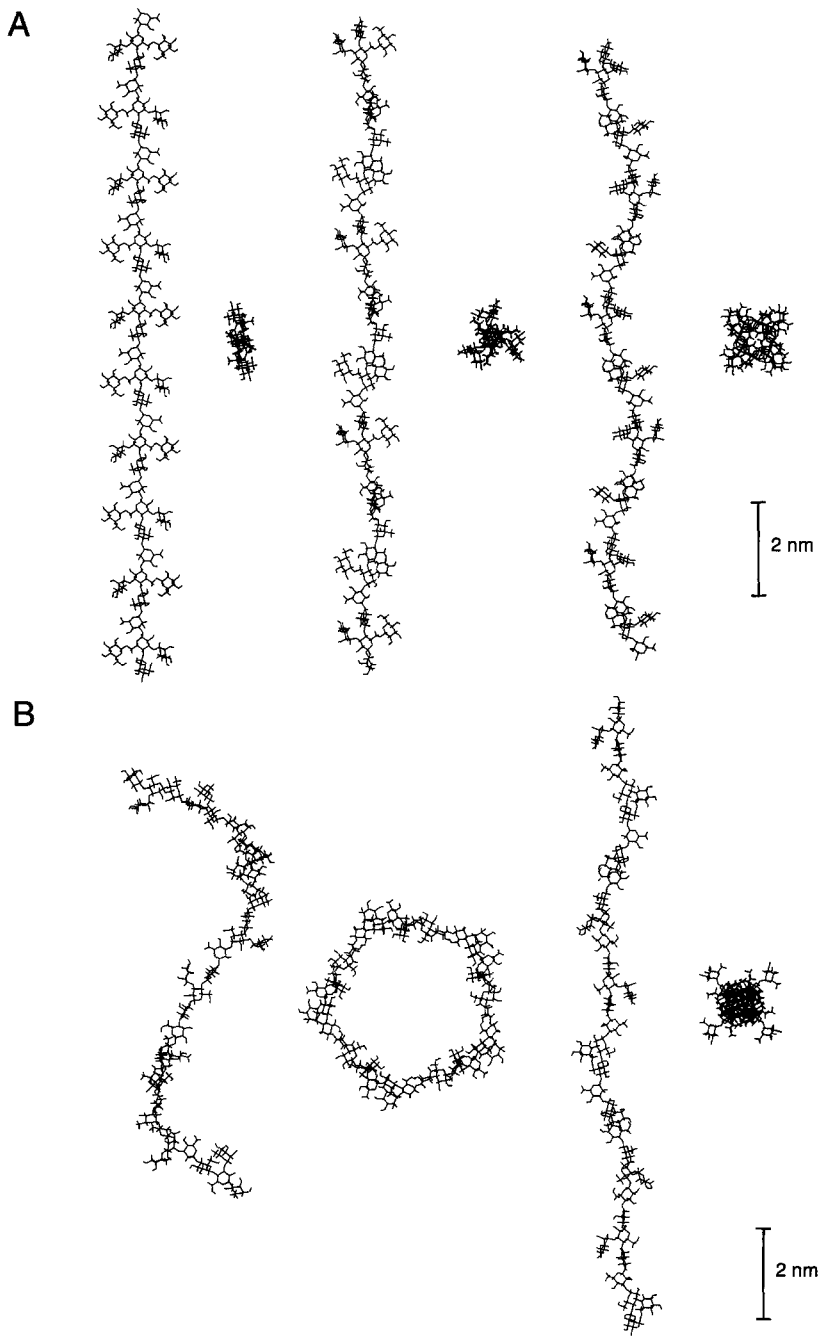

Fig. 6. (A) Helical structures (side- and topview) generated from families 1 (left), 2 (middle), and 3 (right) of the CICADA analysis of **2** and (B) helices generated from families 2 (left) and 4 (right) of the CICADA analysis of **3**. In each case, the polysaccharide chain consists of 30 backbone residues.

structures were generated (Fig. 6B). Extended right- or left-handed symmetries were established from families 1 ($n + 8$, h 2.405 nm) and 4 ($n - 4$, h 2.824 nm) and more hollow, left-handed helices were obtained by extension of families 2 ($n - 5$, h 1.908 nm) and 3 ($n - 6$, h 1.923 nm). Since the repeating backbone structures of the helices derived from the CICADA analyses of **2** and **3** were not defined in the same way (tri- and hexasaccharide structures for **2** and **3**, respectively) the two sets of helical structures derived from **2** and **3** cannot be compared directly. The helices in Fig. 6B can be regarded as composite structures due to the presence of two flexible α-D-Glc*p*-(1 → 3)-β-L-Rha*p* linkages (**C′ → D′** and **C → D**) per hexasaccharide repeating backbone. If the conformations around the **C′ → D′** and **C → D** linkages are not identical, higher order helices are obtained, which exhibit either right- or lefthanded chiralities and are either extented (families 1 and 4; a small difference between the **C′ → D′** and **C → D** conformations) or hollow (families 2 and 3; a relatively large difference between the **C′ → D′** and **C → D** conformations). The generated hollow helical structures give a plausible description of the conformational behaviour of 'kinks' or 'turns' in the polysaccharide chain in solution.

4. Conclusions

The EPS produced by *Lb. sake* 0-1 was examined through molecular mechanics calculations. The relaxed energy maps generated by MM3 of each of the different constituent disaccharides suggest the conformational possibilities and flexibilities of the different glycosidic linkages in the polysaccharide. The α-D-Glc*p*-(1 → 3)β-L-Rha*p* (**C → D**) linkage was shown to be very flexible. A CICADA analysis of a hexasaccharide substructure (**2**) of the EPS demonstrated a total of nine conformational families. However, only three major backbone structures were found, primarily based on variation of the ψ angle of the **C → D** linkage. A CICADA analysis of octasaccharide **3** agreed with the analysis of **2**, although the behaviour of the flexible **C → D** linkage was slightly different, leading to a somewhat different distribution over the different families. Interproton distances obtained from NOESY experiments performed on the *O*-deacetylated, deglycerophosphorylated EPS only partially agreed with the corresponding distances as calculated from the complete ensembles of conformations found by the CICADA calculations. Helical structures generated from the conformational minima of the CICADA analysis of **2** exhibited 2-, 3-, or 4-fold highly extended chiralities. Elongation of the four conformational families of **3** yielded insight into hollow helical structures, illustrating conformational possiblities for 'turns' in the polysaccharide chain in solution.

Acknowledgements

This study was supported by the Dutch Innovation Oriented Research Programme on Carbohydrates (IOP-k) with financial aid from the Ministry of Economic Affairs, the Ministry of Agriculture, Nature Management and Fisheries, the Netherlands Foundation

for Chemical Research (NWO/SON), and Unilever Research Laboratories. Furthermore, we would like to acknowledge the Institut National de la Recherche Agronomique (INRA) and the Centre National de la Recherche Scientifique (CNRS) for their support. The authors would like to thank Dr. S. Cross for skilful assistance with the MM3 calculations. Part of this work has been performed within the CAREnet network which is under the EC Human Capital and Mobility Initiative.

References

[1] P.A. Sandford and J. Baird, in G.O. Aspinall (Ed.), *The Polysaccharides*, Vol. 2, Academic, New York, 1983, pp 411–490.
[2] T. Doco, J.-M. Wieruszeski, B. Fournet, D. Carcano, P. Ramos, and A. Loones, *Carbohydr. Res.*, 198 (1990) 313–321.
[3] H. Nakajima, T. Hirota, T. Toba, T. Itoh, and S. Adachi, *Carbohydr. Res.*, 224 (1992) 245–253.
[4] M. Gruter, B.R. Leeflang, J. Kuiper, J.P. Kamerling, and J.F.G. Vliegenthart, *Carbohydr. Res.*, 231 (1992) 273–291.
[5] M. Gruter, B.R. Leeflang, J. Kuiper, J.P. Kamerling, and J.F.G. Vliegenthart, *Carbohydr. Res.*, 239 (1993) 209–226.
[6] Y. Yamamoto, S. Murosaki, R. Yamauchi, K. Kato, and Y. Sone, *Carbohydr. Res.*, 261 (1994) 67–78.
[7] Y. Yamamoto, T. Nunome, R. Yamauchi, K. Kato, and Y. Sone, *Carbohydr. Res.*, 275 (1995) 319–332.
[8] G.W. Robijn, D.J.C. van den Berg, H. Haas, J.P. Kamerling, and J.F.G. Vliegenthart, *Carbohydr. Res.*, 276 (1995) 117–136.
[9] G.W. Robijn, J.R. Thomas, H. Haas, D.J.C. van den Berg, J.P. Kamerling, and J.F.G. Vliegenthart, *Carbohydr. Res.*, 276 (1995) 137–154.
[10] D.J.C. van den Berg, G.W. Robijn, A.C. Janssen, M.L.F. Giuseppin, R. Vreeker, J.P. Kamerling, J.F.G. Vliegenthart, A.M. Ledeboer, and C.T. Verrips, *Appl. Environm. Microbiol.*, 61 (1995) 2840–2844.
[11] N.L. Allinger, Y.H. Yuh, and J.-H. Lii, *J. Am. Chem. Soc.*, 111 (1989) 8551–8566.
[12] J. Koca, *J. Mol. Struct. (Theochem)*, 308 (1994) 13–24.
[13] J. Koca, S. Pérez, and A. Imberty, *J. Comp. Chem.*, 16 (1995) 296–310.
[14] IUPAC-IUB Joint Commission on Biochemical Nomenclature (JCBN), *Eur. J. Biochem.*, 131 (1983) 5–7.
[15] N.L. Allinger, Y.H. Yuh, and J.-H. Lii, *J. Am. Chem. Soc.*, 112 (1990) 8293–8307.
[16] A.D. French, R.S. Rowland, and N.L. Allinger, in A.D. French and J.W. Brady (Eds.), *Computer modeling of carbohydrate molecules*, Vol. 430, American Chemical Society, Washington DC, 1990, pp 120–140.
[17] A.D. French, V.H. Tran, and S. Pérez, in A.D. French and J.W. Brady (Eds.), *Computer modeling of carbohydrate molecules*, Vol. 430, American Chemical Society, Washington DC, 1990, pp 191–212.
[18] S.N. Ha, L.J. Madsen, and J.W. Brady, *Biopolymers*, 27 (1988) 1927–1952.
[19] M.K. Dowd, P.J. Reilly, and A.D. French, *Biopolymers*, 34 (1994) 625–638.
[20] A. Imberty, S. Pérez, M. Hricovini, R.N. Shah, and J.P. Carver, *Int. J. Biol. Macromol.*, 15 (1993) 17–23.
[21] S. Pérez and M.M. Delage, *Carbohydr. Res.*, 212 (1991) 253–259.
[22] A. Kumar, G. Wagner, R.R. Ernst, and K. Wüthrich, *J. Am. Chem. Soc.*, 103 (1981) 3654–3658.
[23] J.D. Beleja, J. Moult, and B.D. Sykes, *J. Magn. Reson.*, 87 (1990) 375–384.
[24] A.D. French, *Carbohydr. Res.*, 188 (1989) 206–211.
[25] S.B. Engelsen, S. Pérez, I. Braccini, and C. Hervé du Penhoat, *J. Comp. Chem.*, 16 (1995) 1096–1119.
[26] S.B. Engelsen, J. Koca, I. Braccini, C. Hervé du Penhoat, and S. Pérez, *Carbohydr. Res.*, 276 (1995) 1–29.
[27] A. Imberty, E. Mikros, J. Koca, R. Mollicone, R. Oriol, and S. Pérez, *Glycoconjugate J.*, 12 (1995) 331–349.
[28] L.M.J. Kroon-Batenburg, J. Kroon, B.R. Leeflang, and J.F.G. Vliegenthart, *Carbohydr. Res.*, 245 (1993) 21–42.